nature research

https://doi.org/10.1038/s41565-020-00795-y

Supplementary information

Two-dimensional adaptive membranes with programmable water and ionic channels

In the format provided by the authors and unedited

Supporting Information

Two-dimensional adaptive membranes with programmable water and ionic channels

Daria V. Andreeva[1,2], Maxim Trushin[1], Anna Nikitina[1,3], Mariana C. F. Costa[1,2], Pavel V. Cherepanov[1,7], Matthew Holwill[4], Siyu Chen[2], Kou Yang[2], See Wee Chee[5,6], Utkur Mirsaidov[1,2,5,6], Antonio H. Castro Neto[1,2], Kostya S. Novoselov[1,2,4,8]

Preparation and characterization of membranes

We constructed a variety of nanosandwiched materials via the self-assembly of negatively charged 2D polyanion (graphene-oxide (GO) flakes, ~1-2 μm in size), and polycation (positively charged polyamine - PA). The layer-by-layer organization of GO flakes in the membrane is seen in transmission (TEM) and scanning electron microscopy (SEM). Images of the membranes were collected using a FEI Verios460 (ThermoFisher Scientific, USA) field emission SEM at an operating voltage of 2 keV. X-ray diffraction (XRD) patterns (XRD performed using Bruker D8 Advance X-ray transmission diffractometer (Bruker, USA) (CuKα radiation from the copper target using an in built nickel filer, λ = 1.54056 Å) show that an average inter-layer distance between two GO flakes in a nanosandwich is approx. 2 nm. Thus, 250-nm-thick membranes consist of approx. 125 GO-PA-GO layers. The membranes were prepared by vacuum filtration of colloidal solutions of graphene oxide flakes (graphene oxide, 2 mg/mL, dispersion in H_2O, Merck) covered by polyethyleneimine (PEI, branched average Mw ~25,000 by light scattering (LS), branched average Mn ~10,000 by gel permeability chromatography (GPC), (Merck)) and PEI (branched average Mn ~60,000 by GPC, branched average Mw ~750,000 by LS, 50 wt. % in H_2O (Merck)) on two types of filters: Anodisc 47 (pore size – 0.02 μm, diameter 47 mm, Whatman, UK) and polyethersulfon membrane (0.03 μm, 47 mm, Sterlitech Corporation, USA). Colloidal solutions were prepared by mixing of 5 ml of 0.1 mg/ml solution of GO in deionized water at pH 4.6 and 20 ml of 2 mg/ml solution of PEI in 0.1M NaCl at pH 2, 4, 5.5, 9 and 10.2 adjusted by adding 1M HCl solution. pH was controlled by a SevenExcellence pH meter with pH electrode (Mettler Toledo, Switzerland). The colloids were mixed for 5 min using a shaker (rotation speed – 500 rpm, Vortex Mixer, VORTEX-GENIE® 2, USA). Then, the particles were sedimented by centrifugation for 90 min at 2000 rpm, washed by 0.1M NaCl solutions with corresponding pH three times and filtrated under vacuum on a supporting filter to form a film. The filtration process was approx. 2 h. The wet films on filters were dried in a dry cabinet for 24 h before use. GO membranes without polymers were prepared using the same procedure but without polymer. The weight of membranes was measured by weighing the filter, GO membrane without polymer and GO-polymer membranes. The average weight of the membrane without polymer is 1.6±0.2 mg, the average weight of membrane with polymer - 3±0.2 mg. Thus, mass ratio of GO to PEI is 1:1. The thickness was measured by atomic force microscopy (AFM). The thickness is approx. 250±15 nm.

We measured the zeta potential of the membranes using SurPASS 3 Electrokinetic Analyzer (Anton Paar, Germany). The aim was to identify whether negatively charged GO or positively charged PEI forms the outermost layer in the membranes. The zeta potential analysis was done for both the GO-PEI 25kDa membrane assembled at pH 2 and the GO-PEI membrane assembled at pH 10.2. Electrolyte solution: 0.001 mol/l NaCl. pH adjustment: 0.05 mol/l HCl (pH 2-6) and 0.05 mol/l NaOH

(pH 6-10). The results were obtained in the Adjustable Gap Cell for rectangular samples. For each measurement a pair of GO-PEI membranes with same top layer was fixed on the sample holders (with a cross section of 20 x 10 mm^2) using double-sided adhesive tape. The sample holders were inserted in the Adjustable Gap Cell such that the surfaces of the GO-PEI membrane were exactly facing each other. A gap of approx. 100 µm was adjusted between the sample surfaces. An aqueous 0.001 mol/l NaCl solution was used for the zeta potential analysis. Before starting the measurement, the samples were carefully rinsed with the measuring electrolyte. The pH titration was started at pH 8.5 of the 0.001 mol/l NaCl solution (adjusted with 0.05 mol / l NaOH) and commenced towards the isoelectric point (IEP, i.e., pH where zeta potential = 0 mV). The pH was automatically adjusted by the integrated titration unit using 0.05 mol/l HCl and 0.05 mol/l NaOH, respectively. The curves of zeta potentials vs pH for the membranes prepared at pH 2 and pH 10.2 are shown in **Figure S1**. We see that the zeta potentials have negative signs that should be due to the negative surface charge of the membranes formed by negatively charged GO molecules. Thus, the outermost layer of the membranes is formed by GO flakes.

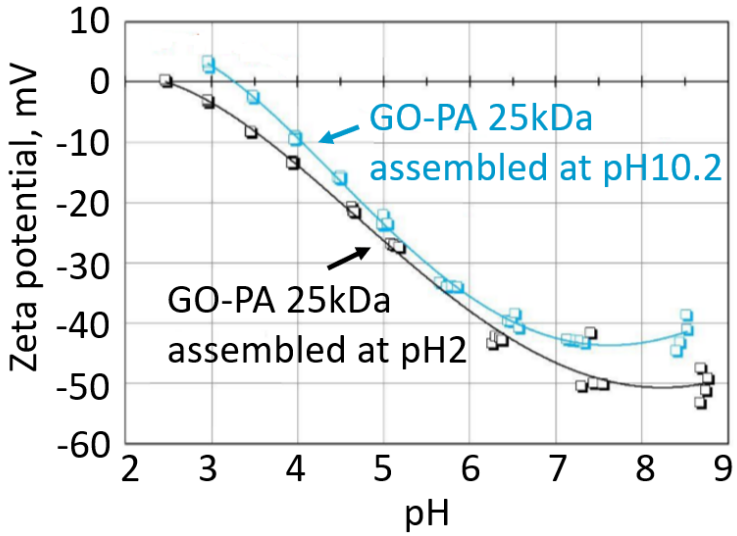

Figure S1. The zeta potential of the surfaces of membranes vs. pH.

TEM, TGA, DSC characterisation

TEM image and the cross section of the layered membrane is shown in **Figure S2**. As well as the thermogravimetry analysis (TGA) the differential scanning colorimetry (DSC).

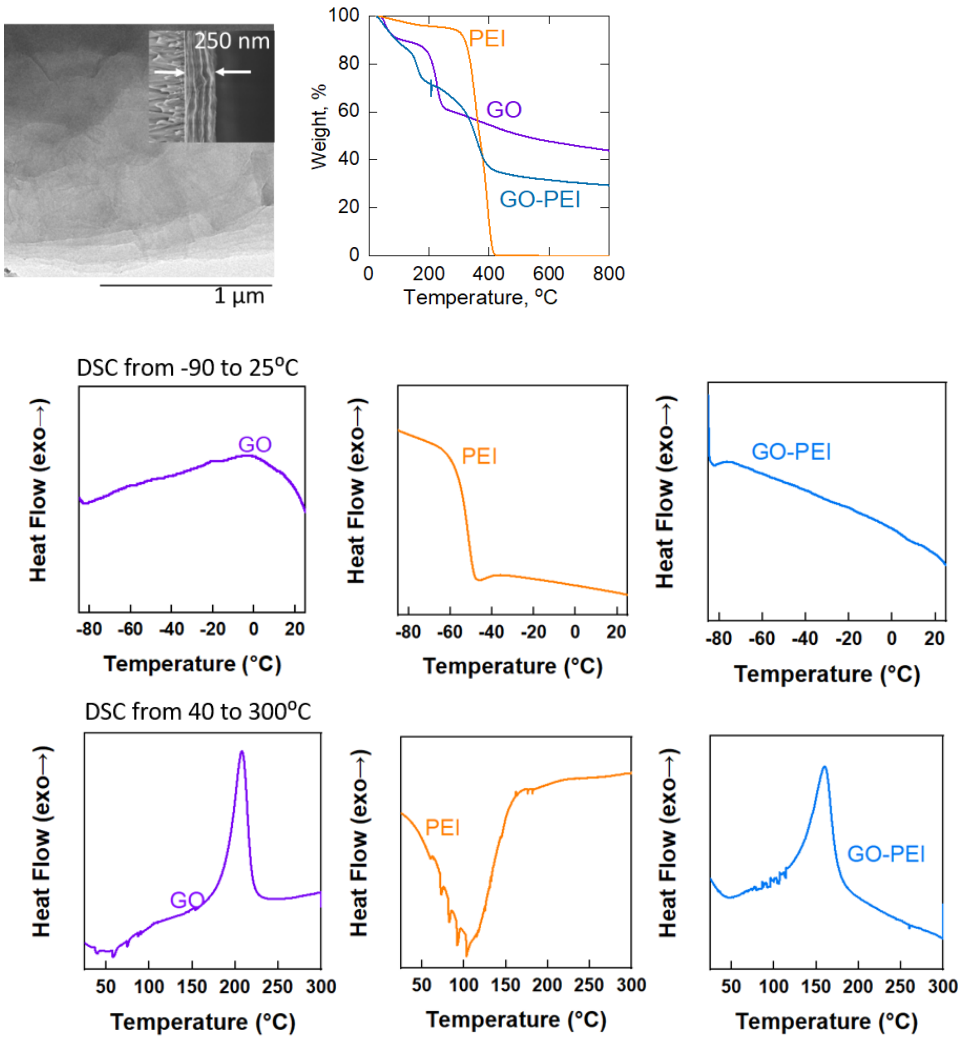

Figure S2. TEM image and the cross section of 250-nm thick membrane on an anodisc filter and TGA (PerkinElmer, heating rate of 10 °C/min in air) and DSC curves of GO, PEI and GO-PEI membrane that shows 1:1 ration of GO and PA in the membrane. GO and GO-PEI membranes were transferred into DSC pans via fishing in deionized water and then were dried in a dry cabinet for 24 hours. PEI was purchased from Sigma Aldrich and used without further purification. DSC was measured by TA Instruments DSC 25 (within the temperature range of -85 °C to 25 °C) and Mettler Toledo DSC1 (within the temperature range of 25 °C to 300 °C) under nitrogen at a heating rate of 10 °C min^{-1}.

AFM characterisation

The thickness of the film can be regulated by concentration of graphene oxide and PA and molecular weight of PA (**Figure S3**).

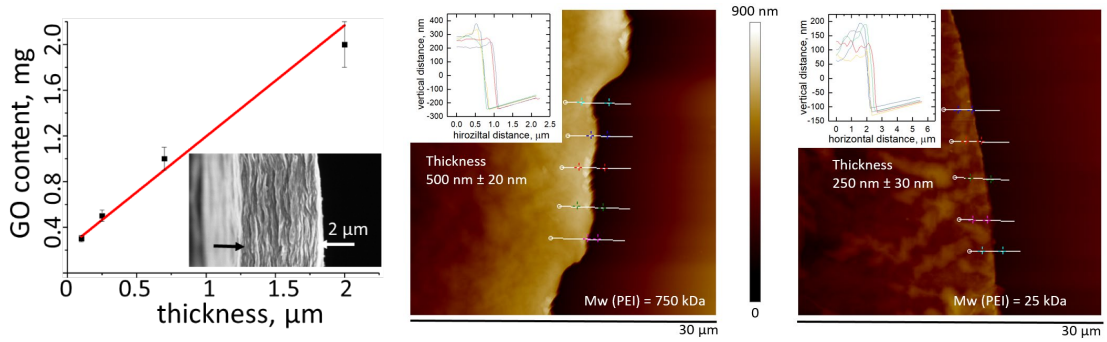

Figure S3. The thickness of GO-PA membrane vs concentration of GO for PA 25kDa (left) AFM images and thickness measurements for GO-PA 750 kDa (middle) and GO-PA 25kDa (right).

X-Ray characterisation

The membrane has a sandwich-like morphology formed by alternating monomolecular layers of PA and GO. X-ray diffraction (XRD) patterns show one narrow peak at 4.6 and one broad peak at 5.4 degree, corresponding inter-layer distances were calculated to be ≈19Å and ≈16Å. Thus, the membranes consist of approx. 125 GO-PA-GO nanosandwiches with inter-layer spacing of approx. 2 nm. It is important that upon swelling interlayer distance doesn't increase; the structure even became slightly more compact in a wet state comparing to a dry state. XRD patterns of the membranes in dry and swollen states and corresponding schematic illustrations of GO-PA-GO sandwiches are shown in **Figure S4**. Remarkably, nanometre-thick GO-PA monomolecular laminates demonstrate excellent stability and maintain integrity in the whole pH range from 1.5 to 12.

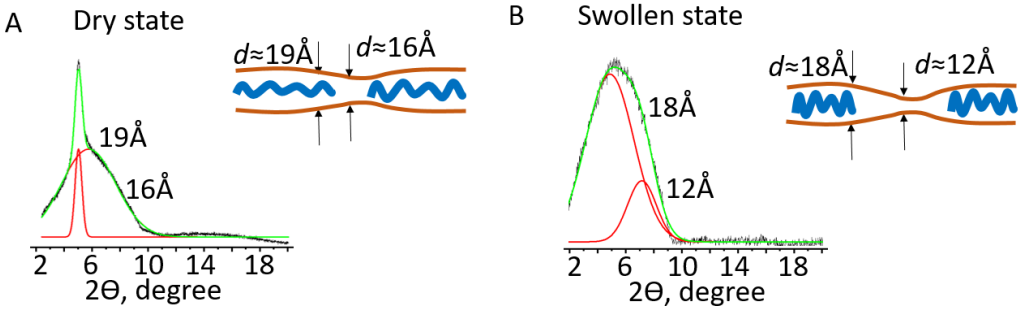

Figure S4. X-ray diffractions of graphene oxide-polyamine membranes prepared at pH 2 in dry (A) and wet (B) states with calculated inter-layer distance (*d*-spacing); inserts – schematic illustrations of structural changes on the membranes upon swelling.

Measurement of surface charge density

Surface charge of GO and PA modified graphene oxide (GO-PA) flakes was estimated using the titration technique. The titrations of 0.5g GO or GO-PA were performed in 0.005 M NaCl background electrolyte. Titrations started either from lower pH (GO dispersion), or higher pH (GO-PA dispersion) with use of 0.1 M NaOH or 0.1 M HCl as base/acid titrants. Both dispersions were titrated in the pH range from 2 to 12. The same procedure was performed for the background electrolyte without presence of GO or GO-PA flakes. Prior to titrations, the dispersions as well as background electrolyte were stirred and purged with N_2 for 30 min to equilibrate and remove any dissolved and adsorbed gases. The titration setup comprises a sample holder, a magnetic stirrer, N_2 gas inlet, acid and base burettes, and a SevenExcellence pH meter with pH electrode (Mettler Toledo, Switzerland). The electrodes were stored, cleaned, activated and calibrated according to the instructions of the manufacturer. Surface charge (σ_s) of GO or GO-PA was calculated using the following equation:

$$\sigma_S(pH) = -F \cdot \frac{\Delta n_{sol,H^+(pH)}}{mA_{sp}}$$

where: *F* - is Faraday constant (*F* = 96500 *C/mol*), *n* - is acid/base balance per sample (*mol*), *m* – sample mass (*g*), A_{sp} – total surface area per one gram (m^2/g); σ_S – surface charge (C/m^2).

The maximum surface charge density was measured to be about -0.2 C/m^2 at pH=11. Distinct from GO, PAs are positively charged. The amino-groups bind protons over a broad pH range and so, the surface charge density increases with an increase in proton concentration. The maximum value of the surface charge can be adjusted by molecular weight (M_w) of PA. The maximum surface charge of PA with M_w of 750 kDa is double the maximum surface charge of PA with M_w of 25 kDa.

Permeability measurements

Water flux was measured using a H1C side-by-side diffusion system equipped with an H1C magnetic stirrer and a heater/circulator. The membrane was placed between two cell halves. In one half, we added 2.5 M solution of sucrose (99%, Merck) in water to create external osmotic pressure (61 Bar). In the second half of the cell we used water solutions at particular pH. pH was adjusted using 1M HCl or 1M NaOH solutions. The permeability tests were conducted for 24 h.

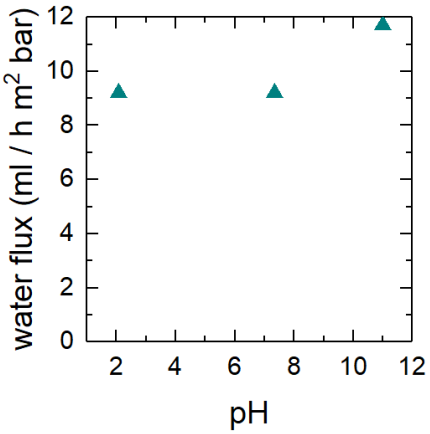

Figure S5. Water flux as a function of pH for GO-PDADMAC membranes.

To experimentally elucidate the function of PA in creating excess osmotic inner pressure in GO membranes we fabricated the following membranes: i) using a positively charged polymer, poly(diallyldimethylammonium chloride) (PDADMAC), whose surface charge density does not depend on pH; ii) with PA having different maximum surface charge densities and, iii) 250-nm thick GO membranes without PA. In order to see the effects, we measured water flux for those membranes at different pH. First of all, the GO-PDADMAC membranes show high permeability for water and the water flux does not significantly depend on pH (**Figure S5**). Both high (750 kDa) and low (25 kDa) M_w PA demonstrate the same tendency in water permeability. The maximum permeability is observed for the high M_w PA due to the higher surface charge density. It is also important that in bare PAs, osmotic pressure can be increased due to the presence of negatively charged chlorides. However, we see in **Figure S5** that the GO-PDADMAC membranes are even more permeable at pH 11 when we do not add chlorides to the system.

Bare GO membranes behave in the opposite way compared to the GO-PA membranes: they are more permeable at basic pH and are less permeable at acidic pH. There are several reasons that such behaviour can be explained: lower permeability of less charged GO flakes at acidic pH in comparison to a more permeable charged membrane at basic pH and; the formation of defected reduced GO structures due to a possible reduction of GO in basic media. Note, that bare GO membranes demonstrate an irreversible switch of permeability. Our experiments show that the nanometer-thick GO membranes prepared without PA are decomposed after one cycle.

Contact angle measurements for the membranes depending on pH and molecular weight of PA

Water contact angle was measured by a KRÜSS DSA25E drop shape analyzer at room temperature. GO-PEI membranes were placed on the stage, and then 9 µL of deionized water at different pH was dropped at the rate of 3 µL/s. Contact angle was automatically measured by the equipment.

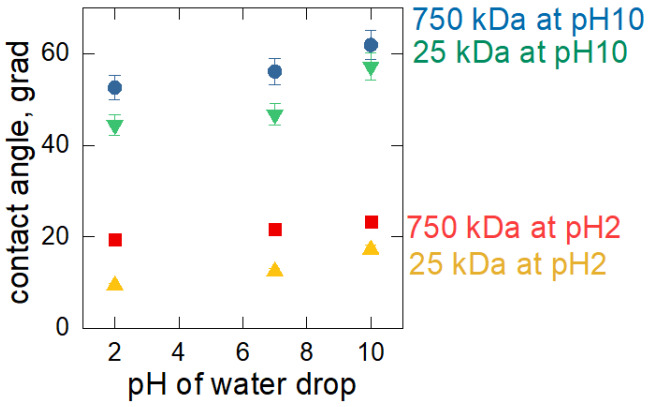

Figure S6. Surface hydrophobicity (contact angle measurements) of the membranes prepared at different pH and using 25kDa and 750 kDa PA.

The water permeability model

The water permeability model is based on the Poisson-Boltzmann, Grahame, and Henderson-Hasselbalch equations [1]. The Poisson-Boltzmann equation describes the spatial charge distribution in the electrolyte. The Grahame equation links the membrane's surface charge, ion density, and electrostatic potential. The Henderson-Hasselbalch equation fits the surface charge as a function of pH. We consider these ingredients in what follows.

Poisson-Boltzmann equation

The electrostatic potential ϕ_x created by an outer graphene-oxide layer of the membrane immersed into a 1:1 electrolyte (e.g. HCl) is determined by the Poisson-Boltzmann equation that reads

$$\frac{d^2\phi_x}{dx^2} = -\frac{e\rho_{\text{out}}^{\infty}}{\epsilon_0\epsilon}\left(e^{\frac{e\phi_x}{k_BT}} - e^{\frac{-e\phi_x}{k_BT}}\right) \tag{S1}$$

where x is the coordinate, ϵ (ϵ_0) are water (vacuum) dielectric constants, T is the temperature, k_B is the Boltzmann constant, $\rho_{\text{out}}^{\infty}$ is the counter-ion concentration far away from the charged plane. This density can be roughly estimated as $\rho_{\text{out}}^{\infty} = N_A 10^{-\text{pH}}$ (dm^{-3}) for acidic solutions without salts added, where N_A is the Avogadro number. Solving equation (S1) one finds that ϕ_x is given by [1]

$$\phi_x = -\frac{2k_BT}{e}\ln\left(\frac{1+\gamma e^{\kappa x}}{1-\gamma e^{\kappa x}}\right), \qquad x < 0, \tag{S2}$$

where $\kappa = \sqrt{2e^2\rho_{\text{out}}^{\infty}/\epsilon_0\epsilon k_BT}$ and $\gamma = \tanh\left(\frac{e\phi_0}{4k_BT}\right)$. The quantity $\frac{1}{\kappa}$ is known as the Debye length. It strongly depends on pH through $\rho_{\text{out}}^{\infty}$. Having solution (S2) at hand we can deduce the spatial dependence of ρ_{out} as

$$\rho_{\text{out}}(x) = \rho_{\text{out}}^{\infty}\mathrm{e}^{-e\phi_x/k_BT}. \tag{S3}$$

Equation (S3) is used to plot the counter-ion densities in **Figure 3** of the main text.

Grahame equation

Equation (S2) determines the x–dependence of the electrostatic potential but it does not contain the surface charge of the layer yet. The GO surface charge σ_{GO} determines the boundary condition $\phi_{x=0} = \phi_0$. The relation between ϕ_0 and σ_{GO} follows from the condition of electroneutrality given by [1]

$$0 = \sigma_{\text{GO}} + \int_{-\infty}^{0} dx e\rho_{\text{out}}^{\infty}\left(\mathrm{e}^{-e\phi_x/k_BT} - \mathrm{e}^{e\phi_x/k_BT}\right), \tag{S4}$$

i.e. the surface charge density must be compensated by the difference between ion and counter-ion concentrations integrated over the whole solution volume. Using equation (S2) the integral can be taken explicitly. Combining the obtained relation with the Poisson-Boltzmann equation we arrive at the Grahame equation given by

$$\frac{\sigma_{GO}^2}{8\epsilon_0\epsilon k_B T\rho_{\text{out}}^{\infty}} = \sinh^2\left(\frac{e\phi_0}{2k_B T}\right). \quad \text{(S5)}$$

Henderson-Hasselbalch equation

The surface charge of GO and GOPA flakes depends on pH-factor of the adjacent solution according to the Henderson-Hasselbalch equation relating the surface charge densities to pK_a's of particular groups [3]. The total surface charge density can be written as

$$\sigma_{\text{GOPA/GO}} = \sigma_{00} \pm \sum_i \frac{\sigma_{0i}}{1+10^{(\pm\mathrm{pH}\,\mp\mathrm{pK}_{ai})}} \quad \text{(S6)}$$

with $\mathrm{pK}_{a1} = 3.55,\ \mathrm{pK}_{a2} = 6.7, \mathrm{pK}_{a3} = 9.4$ for GO, and the values for GOPA are almost the same ($\mathrm{pK}_{a1} = 3.35,\ \mathrm{pK}_{a2} = 6.5, \mathrm{pK}_{a3} = 9.2$). The corresponding charge densities σ_{0i} are determined by fitting experimental curves [4]. In the main text, we have simplified equation (S6) and employed a single pK_a's averaged with the weights given by σ_{0i}. The resulting pK_a for GO/GOPA turns out to be slightly above/below pH-neutrality, and we conveniently fit the measurements depicted in **Figure 2** by the following equation

$$\sigma_{\text{GOPA/GO}} = \frac{\pm\sigma_0}{1+10^{(\pm\mathrm{pH}\,\mp\mathrm{pK}_a)/a}}. \quad \text{(S7)}$$

Here, a is a smearing parameter. However, this approach turns out to be too rough if we want to distinguish the influence of different counter-ions on the surface charge. The fitting values for GO and GOPA in different solutions are summarized in **Table 1** in the section on the ion transport below. The fitting requires a charge shift σ_{00} which is not related to any particular pK_a, and σ_{tot} is defined as a sum of $\sigma_{01}, \sigma_{02}, \sigma_{03}$.

Osmotic pressure and water flow

The inner counter-ion concentration has been estimated in the main text and is shown in **Figure S7** below. The outer counter-ion concentration near the membrane's surface $\rho_{\text{out}}(x=0)$ is shown in the same plot. It is also compared with the bulk concentration far from the membrane. The difference between ρ_{in} and ρ_{out} is maximal near pH2.

The inner excess concentration $\rho_{\text{in}} - \rho_{\text{out}}$ can be translated into the chemical potential difference given by

$$\Delta\mu = k_B T \ln\frac{\rho_{\text{in}}}{\rho_{\text{out}}}. \quad \text{(S8)}$$

The functional dependence $\Delta\mu(\mathrm{pH})$ is demonstrated in **Figure S7**. The osmotic pressure driving the water flow is assumed to be proportional to $\Delta\mu$. The corresponding fitting function is given in the **Figure caption 2** of the main text.

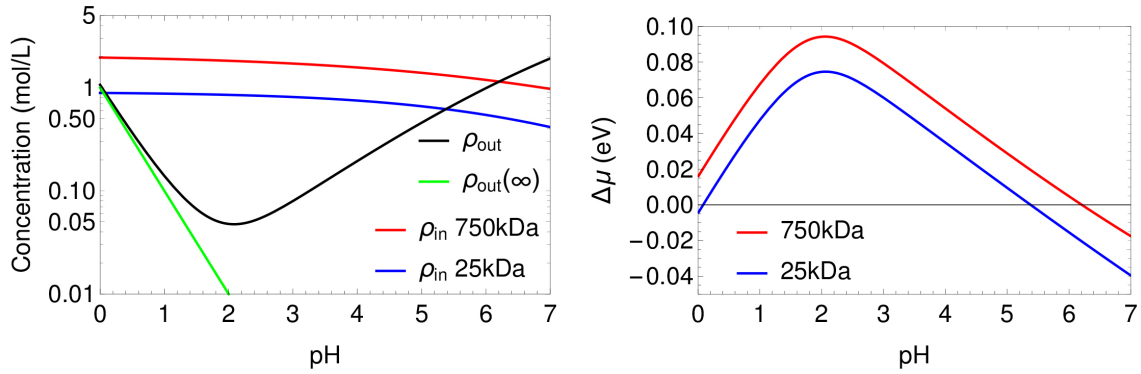

Figure S7. Left panel: The inner and outer counter-ion concentrations as compared with the concentration in the solution far from the membrane ($T = 300$ K, $\epsilon = 80$). Right panel: The chemical potential difference given by equation (S8).

Quartz-Crystal Microbalance (QCM)

Quartz-Crystal Microbalance (QCM) measurements were performed on AWS A20 system (BioLogic, France) using Ti/Au polished finish 5 MHz resonators. Before each measurement QCM resonators were cleaned with Piranha solution. For electrochemical QCM (e-QCM) measurements the AWS A20 system was coupled with a potentiostat/galvanostat SP300 (BioLogic, France). We used three-electrode electrochemical cell. Ti/Au resonator served as a working electrode. Pt-wire was a counter electrode. Ag/AgCl(3MKCl) was used as reference electrode. 0.1 M NaCl was used as an electrolyte.

We measured a degree of swelling of the membranes assembled at different pH using quartz crystal microbalance (QCM). The kinetics curves in **Figure 2D** show that the membrane entraps water at acidic pH and loses water at basic pH. This is reasonable because at higher concentration of protons, excess osmotic pressure forces water transport into the membranes. However, X-ray diffraction (XRD) patterns reveal almost no changes in interlayer distances in the membranes in wet states compared to those in dry states. Furthermore, inter-layer distances of the membranes do not change upon the membranes' use at different pH.

The reversibility of swelling/shrinking process is shown in **Figure S8.** The membranes reversibly swell at acidic pH and shrink at basic pH. It is demonstrated for at least 3 cycles.

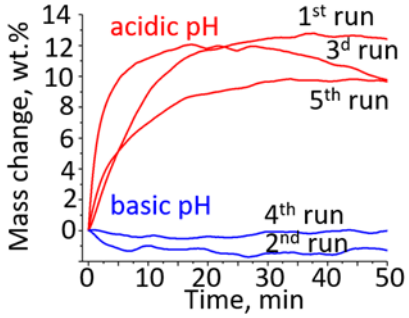

Figure S8. Swelling/shrinking cycles for GO-PA membrane.

In-situ liquid cell TEM experiments

The in-situ liquid cell experiments were performed in a 200kV JEOL 2010F field-emission TEM (Tokyo, Japan) and with a Hummingbird Scientific liquid flow holder (Lacey, WA, USA). Silicon chips with 30 nm thick silicon nitride membrane windows were used to form the microfluidic cell. The GO-PA films were transferred onto one of the liquid cell chips and the chip was allowed to dry. Then, the liquid cell was assembled, and the holder was loaded into the TEM. During imaging, a low electron flux of 1-2 e-/Å2·s to minimise beam induced damage to the nanosandwich. Water was introduced into the liquid cell using the external fluid tubing and syringe pump. In situ movies were collected using a Gatan OneView-IS camera (Pleasanton, CA, USA). For the pH4 sequence, the images were collected at regular time intervals, rather than continuous imaging to reduce the electron fluence to the sample. The electron beam was blanked in between.

To show that pH can be used to program the dynamic properties of the membranes, we apply liquid cell TEM to directly visualize the dynamics of GO flakes when water is introduced to membranes prepared at different pH. **Figure S9** shows TEM micrographs of GO-PA membranes prepared at pH 7 (less charged PA) and pH 4 (more charged PA). The first set of images show dry surfaces, and the following set of images the same surfaces are shown after water starts flowing in the cell. In the upper sequence, we see how a water droplet spreads in the membrane prepared at pH 7. At t = 30 sec, the wrinkled GO flakes unfolded. Unfolding of the membrane prepared at pH 4 is visible after 60 min only. Therefore, the membranes assembled at pH 7 consume water and exhibit faster structural changes to confirm that the unfolding is indeed due to consumed water.

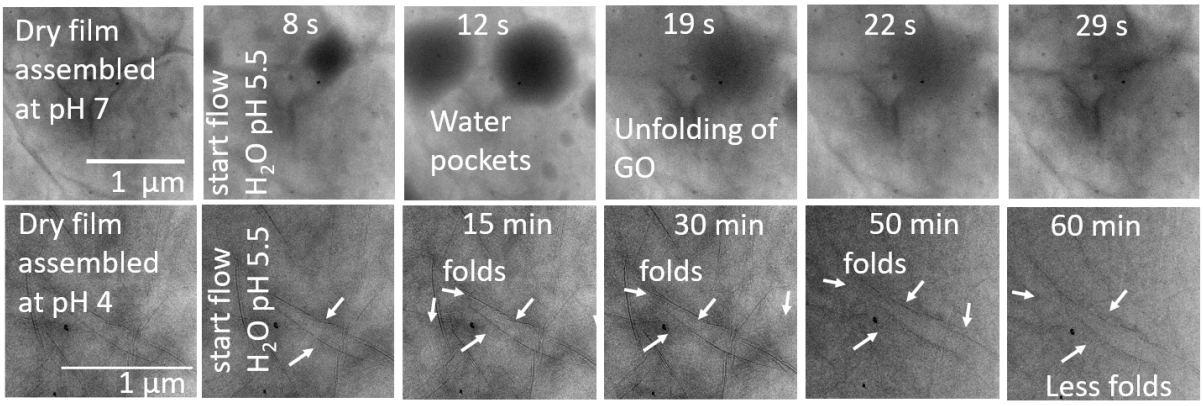

Figure S9. Transmission electron microscopy images recorded using liquid cell with water flow shows unfolding of wrinkled GO flakes upon water treatment. The folds are highlighted by arrows. The membrane prepared at pH 7 is unfolded within 30s. The membrane prepared at pH 4 shows less folds after 1h of water flow.

Ion permeability through GO-PA 750 kDa membranes

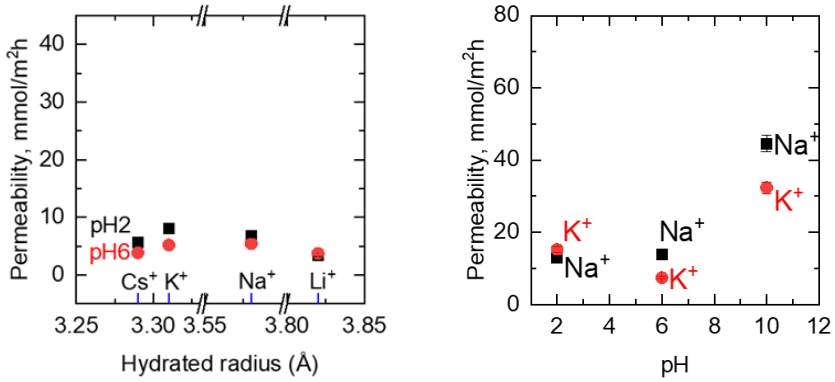

Figure S10. Ionic permeability vs. the hydrated radii of ions for the 0.1M mixture of ions adjusted to pH 2 and pH 6 (left) and ionic permeability of GO-PA membranes as a function of pH measured separately for K^+ and Na^+ (right) for the membrane prepared with 750 kDa PA.

Ion permeability through GO membranes and GO-PDADMAC membranes

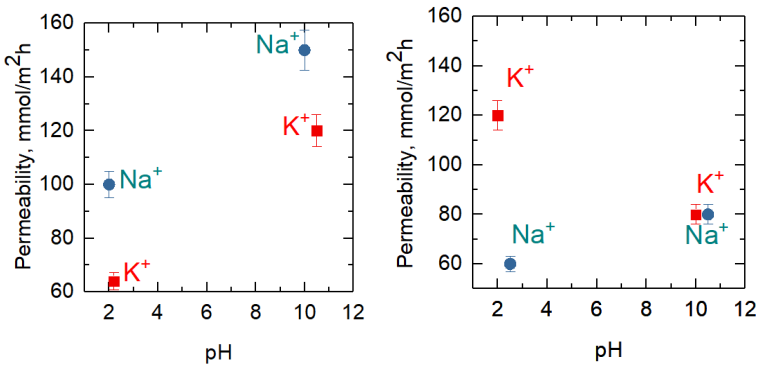

Figure S11. Ionic permeability of GO membranes (left) and GO-PDADMAC membranes (right) as a function of pH for K^+ and Na^+. We used 0.1M solutions of corresponding chloride salts adjusted to a particular pH. The pH range was from 2 to 10. The membranes were tested under reverse osmosis conditions against 2.5M sucrose solution. The experimental time was 24h.

Concentration of ions inside of the membrane (ICP)

Concentration of ions in membranes was tested by Perkin Elmer Avio 500 ICP-OES. Free standing membranes were immersed in 5 mL 0.1M salt solutions (CsCl, KCl, NaCl, LiCl) for 24 h. Membranes were taken out and dried in a dry cabinet overnight. Before concentration analysis, the above membranes were digested with HNO_3/HCl (3:1) in microwave at 240 °C for 15 mins and top up to 10 mL with H_2O. Clear solution was observed prior to ion concentration analysis. The results are shown in **Figure S12**. The concentration of K^+ is at least one order of magnitude higher than the concentrations of Na^+ and Li^+ ions. Cs^+ ions were not detected.

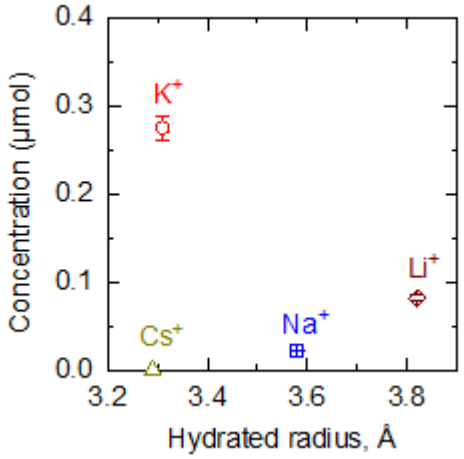

Figure S12. Concentration of ions in the membrane measured by ICP. The membranes were immersed for 24h in 0.1M solutions of corresponding salts.

Attenuated total reflectance Fourier transform infrared (ATR-FTIR) spectroscopy

Attenuated total reflectance Fourier transform infrared (ATR-FTIR) spectra were obtained from Bruker Alpha Platinum-ATR tool. The measured films of GO, PA and the GO-PA membranes prepared at pH 10.2. The most interesting for us is the 1598-1640 cm^{-1} spectral range which corresponds to carbonyl groups of GO. Surprisingly, the intensity of peaks in this region became much more pronounced after the formation of GO-PA composites.

X-ray photo electron spectroscopy (XPS)

X-ray photo electron spectroscopy (XPS) measurements were carried out using a PHI 5000 VersaProbe. The results indicate an increase in intensity from carbonyl groups after the formation of GO-PA composites.

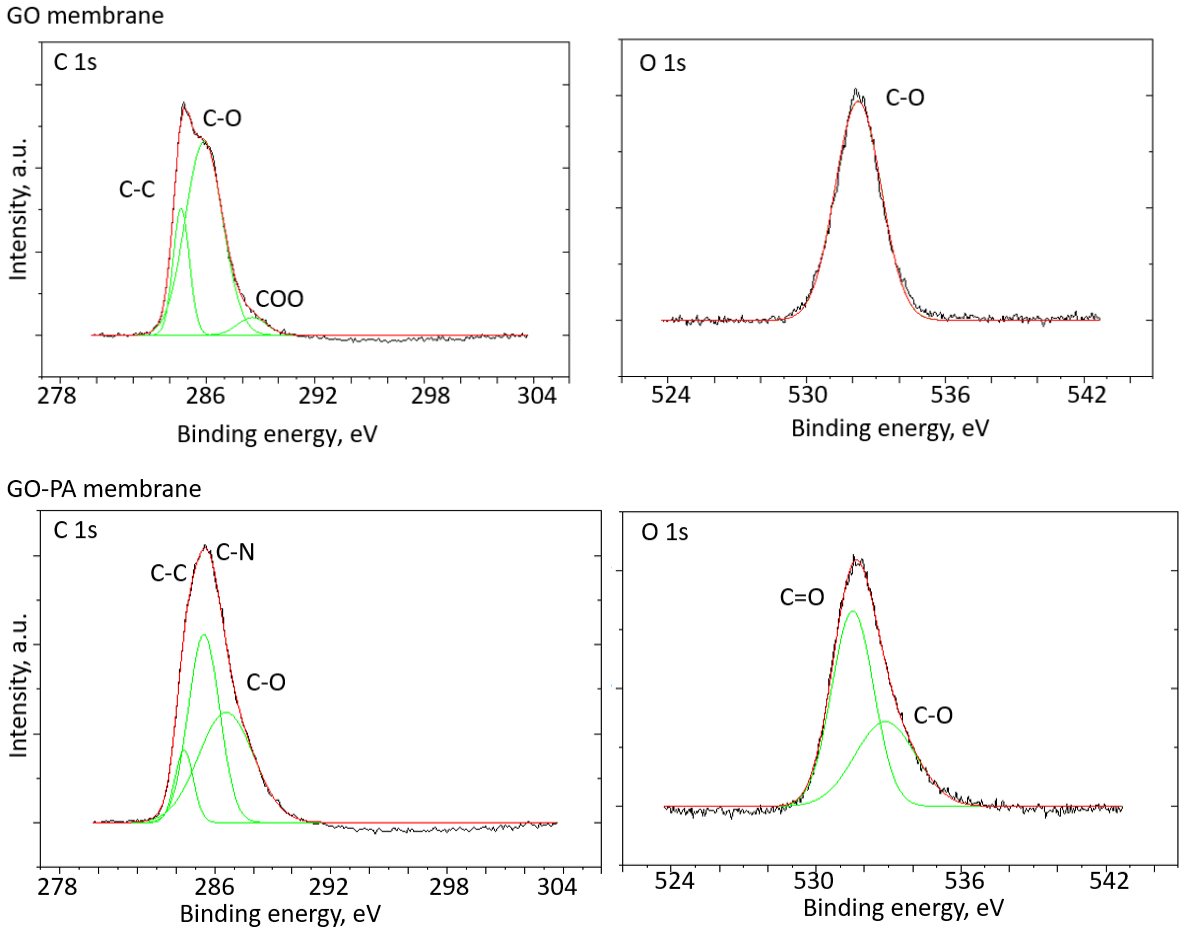

Figure S13. The high-resolution XPS spectra of C 1s and O 1s in the GO and GO-PA membranes.

Effect of K^+ on the permeability of Na^+

We measured ion permeability for K^+ depending on K^+ concentration and also effect of K^+ concentration on permeability for Na^+ in K^+/Na^+ mixtures. Corresponding amount of KCl was dissolved in 20 mL water to prepare different solution concentrations (left panel in **Figure S14**). The concentration of Na^+ in K^+/Na^+ mixtures was adjusted by adding corresponding amount of NaCl (right panel in **Figure S14**). The permeability tests were conducted for 24 h. We see that the permeability for K^+ increases with the K^+ concentration. The similar permeability was measured at 0.5M and 1M concentrations. A dramatic increase in K^+ permeability is expected, as the partial ion pressure driving the K^+ flow is also increasing with the ion concentration in the feed solution. However, an increase in the concentration of K^+ doesn't significantly affect the permeability for Na^+. It is still very low because neither number of hopping sites for Na^+ nor Na^+ concentration in the feed solution change in this set of measurements. The measurements support the hypothesis about the presence of K^+ selective sites in the membranes.

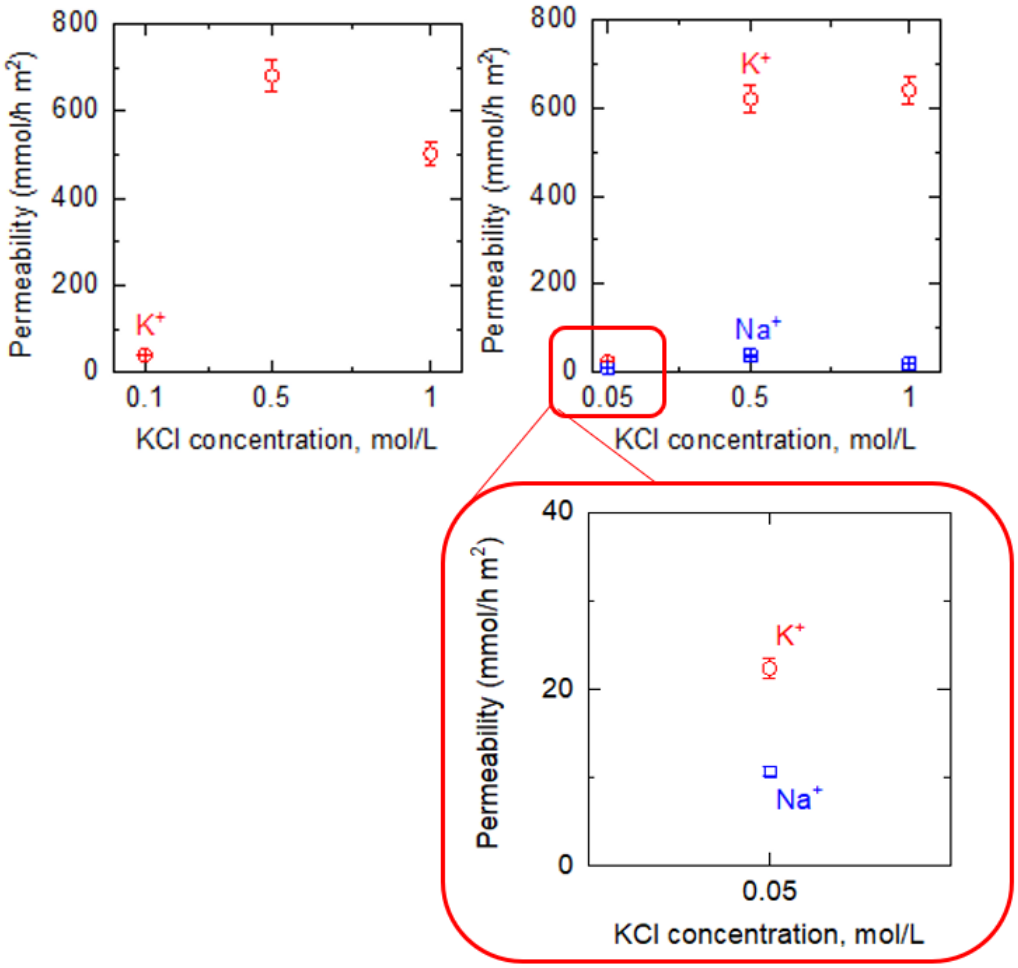

Figure S14. Permeability for K^+ vs. K^+ concentration (left). Permeability for K^+ and Na^+ in K^+/Na^+ mixtures (right). We used the fixed concentration for Na^+ (0.05M solution) in the feed solution, where pH2 is maintained. The concentration of K^+ in the feed solution was varied from 0.05M to 1M. The insert (below) shows the permeability of K^+ and Na^+ ions at 0.05M/0.05M ratio.

The ion transport model

The ion transport model is based on the Oosawa-Manning concept that classifies the counter-ions into two categories: counter-ions freely moving outside potential valleys of a charged structure and counter-ions localized near the structure backbone [2]. In our case, negatively charged GO planes represent the structure backbone, and K^+, Na^+, Cs^+, Li^+, and H^+ are the counter-ions. Since we have a few species of counter-ions the configuration entropy starts playing a role, and hopping transport becomes possible. The details of the model are given in the following sections.

Table S1 indicates that K^+ ions substantially change titration curves: both GO and GOPA accumulate highest surface charge when K^+ ions appear in solution. The strongest difference is observed in σ_{03} for GO (highlighted by bold). The titration curves are plotted in **Figure S15** below. The titrations of 0.1 mg/ml GO and GO-PA were performed in the presence of either 0.1 M salt solutions or without salt at all. Titrations started from basic pH (≈ 11) with use of 0.1 M corresponding base. 0.1 M HCl was used as titrant. Titration solution was stirred using a magnetic stirrer. The pH was measured by a SevenExcellence pH meter with a pH microelectrode (Mettler Toledo, Switzerland). The microelectrode was stored, cleaned, and calibrated according to the instructions of the manufacturer.

Table S1. The charge densities used to fit titration curves for GO and GOPA, see equation (S6) for notations.

GO in	σ_{00} (C/m^2)	σ_{01} (C/m^2)	σ_{02} (C/m^2)	σ_{03} (C/m^2)	σ_{tot} (C/m^2)
KOH	0	-0.04	-0.07	**-0.125**	-0.235
KCl	-0.02	-0.04	-0.07	0	-0.11
NaOH	-0.075	-0.025	-0.045	-0.025	-0.095
NaCl	-0.025	-0.035	-0.055	-0.04	-0.13
LiOH	-0.045	-0.03	-0.05	-0.045	-0.125
LiCl	-0.035	-0.03	-0.05	-0.045	-0.125
CsOH	-0.02	-0.02	-0.075	-0.05	-0.145
CsCl	-0.02	-0.04	-0.05	-0.03	-0.12
GOPA in	σ_{00} (C/m^2)	σ_{01} (C/m^2)	σ_{02} (C/m^2)	σ_{03} (C/m^2)	σ_{tot} (C/m^2)
KOH	0	0.08	0.08	0.15	0.31
KCl	0.055	0.08	0.08	0.15	0.31
NaOH	0	0.04	0.055	0.09	0.185
NaCl	0.01	0.04	0.055	0.09	0.185
LiOH	0	0.08	0.08	0.13	0.29
LiCl	0.01	0.06	0.08	0.13	0.27
CsOH	-0.01	0.095	0.085	0.1	0.28
CsCl	-0.03	0.075	0.085	0.1	0.26

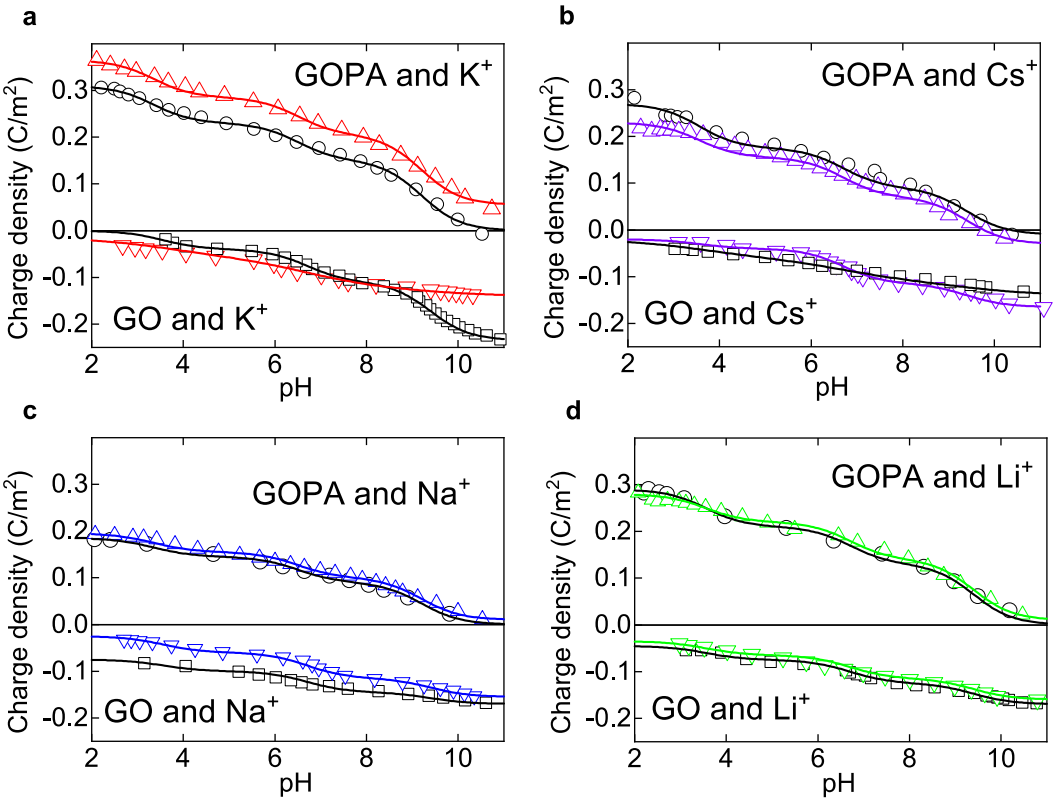

Figure S15. Titration curves for GO and GOPA converted into the surface charge (cf. **Figure 2B** in the main text) and fitted by equation (S6) with parameters given in **Table S1**. Black/colour curves represent titration without/with the respective salt. Note the strong offset between black and colour curves in the presence of K^+.

<u>Ion permutations and potassium transport</u>

If we have more than one counter-ion species condensed near GO backbone, then the ions can exchange and hopping transport may occur. The transport efficiency is then quantified by the number of permutations, W. If we have just two counter-ion species (say, K^+ and H^+), then the permutation number reads

$$W = \frac{(n_{K+} + n_{H+})!}{n_{K+}!\, n_{H+}!}, \tag{S9}$$

where n_{H+} and n_{K+} are the numbers of condensed protons and potassium ions, respectively. Equation (S9) can be easily generalized to any number of ion species involved. If all ion species can exchange with each other with the same probability, then the permutation number reads

$$W_{\mathrm{mix}} = \frac{(n_{H+} + n_1 + n_2 + \ldots + n_N)!}{n_{H+}!\, n_1!\, n_2! \ldots n_N!}, \tag{S10}$$

where n_i is the number of ions of a kind. Note, however, that equation (S10) should be used with care, as not every kind of ion is able to exchange with any other. In what follows, we make use of equation (S9) to describe transport of condensed K^+ ions due to permutations with protons.

The ion permeability is assumed to be proportional to the configuration entropy, hence, to $\ln W$. The latter can be transformed using the Sterling formula as

$$\ln W \approx n_{K+} \ln(1 + \frac{n_{H+}}{n_{K+}}) + n_{H+} \ln(1 + \frac{n_{K+}}{n_{H+}}). \quad \text{(S11)}$$

The numbers n_{K+} and n_{H+} can be written in terms of respective charge densities, and the resulting potassium permeability then reads

$$P_{K+} = \frac{1}{eN_A\tau_{K+}}\left[\sigma_{K+} \ln(1 + \frac{\sigma_{H+}}{\sigma_{K+}}) + \sigma_{H+}\ln(1 + \frac{\sigma_{K+}}{\sigma_{H+}})\right] \left(\frac{\text{mol}}{\text{h} \cdot \text{m}^2}\right), \quad \text{(S12)}$$

where e is the elementary charge, N_A is the Avogardo number, and $\tau_{K+} \sim 5.5 \cdot 10^{-5}$ (h) is the fitting time-scale determined by the average channel length, hydrated ion radius, and driving partial pressure.

The remaining task is to estimate σ_{H+} and σ_{K+} condensed in the interlayer channels. The latter can be roughly estimated as the difference in titration charges σ_{tot} in the absence and presence of salt, see **Table S1**. It is by far the largest in the potassium case (comparable with σ_{tot} itself) and most likely associated with the carbonyl groups. The remaining counter-ion charge condensed on the interface is due to protons, i.e. $\sigma_{H+} = \sigma_{\text{GOPA}} - \sigma_{K+}$, where σ_{GOPA} is given in **Figure S15(a)** (fitted by parameters in **Table S1**). Equation (S12) is used to plot the fitting curves in **Figure 4A** of the main text with σ_{K+}= 0.2 (C/m^2). Note, that in extremely acidic solutions protons may partially substitute K^+ ions inside the membrane that reduces their permeability. Transport of the ions other than K^+ is strongly suppressed due to inability to swap with H^+, as one can see in **Figure S15(bcd)** and **Figure 4DE** even by the naked eye.

<u>Mixing ions for more efficient permeability</u>

Permeability of Cs^+, Na^+, and Li^+ is only efficient in the presence of K^+. Let us denote either of the ion species other than K^+ and H^+ by X^+. The ions X^+ can exchange with K^+, but cannot with H^+. To estimate permeability of K^+ and X^+ in a mixture of both we make use of equation (S10). The permutation number for K^+ in the presence of X^+ is $W_{K+} = (n_{H+} + n_{K+} + n_{X+})!/(n_{H+}!\, n_{K+}!\, n_{X+}!)$, and the permutation number for X^+ in the presence of K^+ is $W_{X+} = (n_{K+} + n_{X+})!/(n_{K+}!\, n_{X+}!)$. Taking logarithm of W_{K+} and W_{X+} we derive the corresponding permeabilitys in the same way as in the previous section:

$$P_{K+} = \frac{1}{eN_A\tau_{K+}}\left[\sigma_{K+} \ln(1 + \frac{\sigma_{H+} + \sigma_{X+}}{\sigma_{K+}}) + \sigma_{H+}\ln(1 + \frac{\sigma_{K+} + \sigma_{X+}}{\sigma_{H+}}) + \sigma_{X+}\ln(1 + \frac{\sigma_{H+} + \sigma_{K+}}{\sigma_{X+}})\right] \left(\frac{\text{mol}}{\text{h} \cdot \text{m}^2}\right),$$
$$P_{X+} = \frac{1}{eN_A\tau_{X+}}\left[\sigma_{K+} \ln(1 + \frac{\sigma_{X+}}{\sigma_{K+}}) + \sigma_{X+}\ln(1 + \frac{\sigma_{K+}}{\sigma_{X+}})\right] \left(\frac{\text{mol}}{\text{h} \cdot \text{m}^2}\right). \quad \text{(S13)}$$

The permeability for K^+ turns out to be always higher than for X^+ as long as the channels are protonized (assuming $\tau_{K+} \sim \tau_{X+}$). The permeability for X^+ remains finite as long as K^+ ions are provided for exchange. If one assumes roughly equal concentrations of X^+, K^+, and H^+ inside the channels ($\sigma_{H+} \sim \sigma_{K+} \sim \sigma_{X+}$), then the ratio between permeabilitys for K^+ and X^+ turns out to be a little higher than 2. This is what one can see in **Figure 4C** in the main text: despite the permeability of K^+ and Cs^+ changes with time its ratio indeed remains very close to 2. Moreover, the ratio between permeabilities for K^+ and Na^+ is also about 2, as long as the feeding concentrations of both ion species are equal, see **Figure S14**. The model is further illustrated in **Figure S16** below.

In the previous paragraph we have assumed that the driving concentration gradients are the same for both ion species that results in $\tau_{K+} \sim \tau_{X+}$. Once we change the feeding concentration of a given ion specie the corresponding τ changes in accordance with the theory of one-dimensional random walk, see **Figure S17**. Let τ_0 be the time required to perform a single hop (this characteristic time

does not depend on direction). The hopping may occur in two possible directions: forward with the probability p and backward with the probability q. (Note that $p + q = 1$.) The total time required to get along the chain of the length N (here, N is just the number of sites in the chain) can be written as

$$\tau = \frac{N\tau_0}{p-q},\ p \geq q. \qquad \text{(S14)}$$

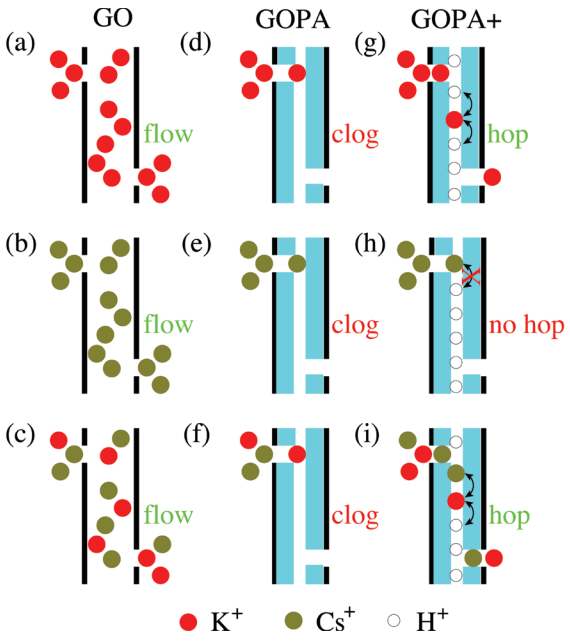

Figure S16. Ion transport overview assuming that K^+ can exchange with Cs^+ and H^+ in PA transport channels, but Cs^+ can exchange with K^+ only. (a)–(c) Ionic flow through pure GO interlayer gap is always possible. (d)–(f) K^+ and Cs^+ are stuck in PA interlayer filling and the transport channel is clogged as long as PA is not protonated. (g) Protonation creates a hopping channel through PA allowing for K^+ transport. (h) Cs^+ cannot efficiently exchange with H^+, as our titration curves suggest, hence no Cs^+ hopping transport occurs. (i) A mixture of K^+ and Cs^+ can get through the protonated channel but K^+ can do that more efficiently.

Equation (S14) can be derived using so-called *the monkey on the cliff* problem in the theory of random walks, see any textbook on the topic, e.g. [5]. Let us now consider the permeability of K^+ ions upon gradual increase of their concentration in the feeding solution. In the equilibrium $p = q = 1/2$, and $\tau_{K+} \to \infty$ making P_{K+} vanish. Increasing concentration K^+ in the feeding solution above 0.5M results in the strongly preferred hopping direction along the chain towards the end with lower concentration, hence, $p \to 1$ and $q \to 0$, and $\tau_{K+} \to N\tau_0 \sim 10^{-5}$ (h). This is the minimal τ_{K+} possible within the model of random walks for a given $N\tau_0$. Hence, no further increase of K^+ permeability with K^+ feeding concentration is possible as long as σ_{K+} or σ_{H+} do not change. This is what we observe in **Figure S14**. At moderate K^+ concentrations of about 0.05M we estimate τ_{K+} to be 25 times longer than at 0.5M that suggests $p = 0.52$ and $q = 0.48$ in this regime.

The permeability of X^+ ions does not change when K^+ feeding concentration increases because the partial gradient for X^+ ions stays the same (τ_{X+} does not change). This is what we see in **Figure S14**: Na^+ permeability fluctuates by factor of 2 despite drastic changes in K^+ concentration by one order of magnitude.

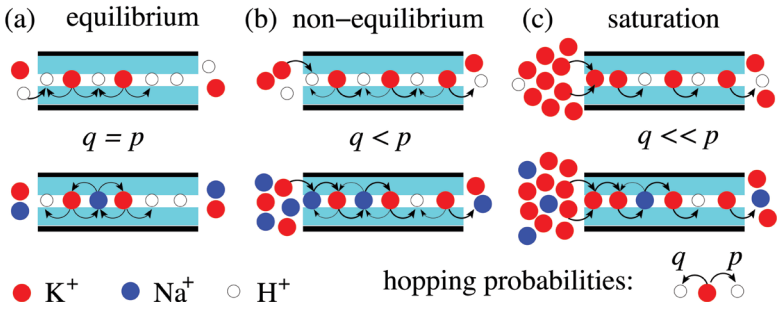

Figure S17. Ion transport at different concentration gradients along the channel. (a) If the ion concentrations are equal at both ends of the channel, then the hopping probabilities are the same in both directions. As a consequence, the transport rate is negligible (i.e. τ is infinite). (b) In the case of moderate ion concentration difference (about 0.1M) the hopping probabilities are asymmetric and τ becomes finite. Note, however, that K^+ can exchange with both H^+ and Na^+, but Na^+ can swap with K^+ only. This is the reason why permeability of K^+ is always more efficient than that of Na^+ even though the driving concentration gradient may be the same for both ion species (i.e. equal τ's), as shown in the lower panel. (c) In the case of high ion concentration difference (about 1M) the hopping probability is strongly asymmetric ($q \to 0, p \to 1$), so that K^+ jumps forward only. This maximizes the transport rate, hence, minimizing τ ($\tau \to N\tau_0$, where τ_0 is the single hopping time, and N is the number of hopping sites in the chain). Since further decrease of τ is not possible the permeability of K^+ saturates in this regime. The permeability of Na^+ remains of the same order of magnitude as in (b) because the driving concentration gradient does not change.

References

[1] Israelachvili, J. N. *Intermolecular and Surface Forces* (Elsevier, 2011).
[2] Dobrynin, A. V. & Rubinstein, M. *Progress in Polymer Science* **30**, 1049 (2005).
[3] Katchalsky, A. & Spitnik, P. *Journal of Polymer Science* **2**, 432-446, (1947).
[4] Orth, E.S. *et al. Journal of Colloid and Interface Science* **467**, 239 (2016).
[5] Feller, W., *An Introduction to Probability Theory and Its Applications*, Third edition, (Wiley, 1968).